A mitochondrial regulon for developmental ferroptosis in rice blast

Qing Shen[1], Fan Yang[1], Naweed I. Naqvi[1,2,*]

[1]Temasek Life Sciences Laboratory, 1 Research Link, Singapore, 117604.
[2]Department of Biological Sciences, National University of Singapore, 16 Science Drive 4, Singapore 117558.

*For correspondence: Naweed I. Naqvi (naweed@tll.org.sg), +65 68727493.

Summary

Ferroptosis, an iron-dependent demise driven by lethal levels of intracellular lipid peroxides, precisely regulates cell death in spores or conidia of the fungal pathogen *Magnaporthe oryzae,* and subsequently determines its ability to cause the destructive blast disease in rice. Despite its importance, little is known about the molecular mechanisms underlying such developmental cell death in fungi. Here, through gene deletion(s) or pharmacological inhibition, we establish a specific functional correlation between ferroptosis and mitochondrial degradation via mitophagy. The requirement of mitophagy for accumulation of lipid peroxides and thus ferroptosis was further attributed to its ability to maintain a pool of metabolically active mitochondria. Disrupting the electron transport chain or decreasing the mitochondrial membrane potential caused mitochondrial fusion and inhibited ferroptosis, thus simulating the loss of mitophagy phenotypes. Graded inhibition of Coenzyme Q (CoQ) biosynthesis in the presence or absence of the lipophilic antioxidant Liproxstation-1 further distinguished the antioxidant function of CoQ from its roles in electron carrier and membrane potential. Such membrane potential-dependent regulation of cellular iron homeostasis and ATP synthesis further linked mitochondrial metabolism to ferroptosis. Rather surprisingly, loss of mitochondrial β-oxidation of fatty acids for acetyl-CoA generation, had no effect on mitochondrial membrane potential and ferroptosis in conidial cells. Therefore, metabolically active mitochondria capable of undergoing precise mitophagy are necessary for fungal ferroptosis. Together, results here reveal a novel mitochondrial regulon for ferroptosis, occurrence of which enables *M. oryzae* in timely establishment and spread of the devastating blast disease in rice.

Key words

Cell death, Iron, Ferroptosis, Mitophagy, Mitochondrial membrane potential, Electron transport chain, Coenzyme Q10, Rice blast, Pathogenesis.

New Results

Ferroptosis, an iron-dependent cell death conserved from fungi to plants and human[1], is caused by increased peroxidation of polyunsaturated fatty acid (PUFA) containing membrane lipids[1,2]. For example, highly regulated cell death in 3 conidial cells of the rice blast fungus *Magnaporthe oryzae* is executed by ferroptosis, and represents a crucial determinant of pathogenic development and infection ability leading to the destructive rice blast disease[2,3]. Such developmental cell death initiates sequentially in the terminal, middle and proximal cell of the conidium in *M. oryzae* (**Figure 1a**)[3], during initiation and maturity of the infection structure called appressorium at the tip of the germ tube that emanates from the proximal conidial cell (**Figure 1a**).

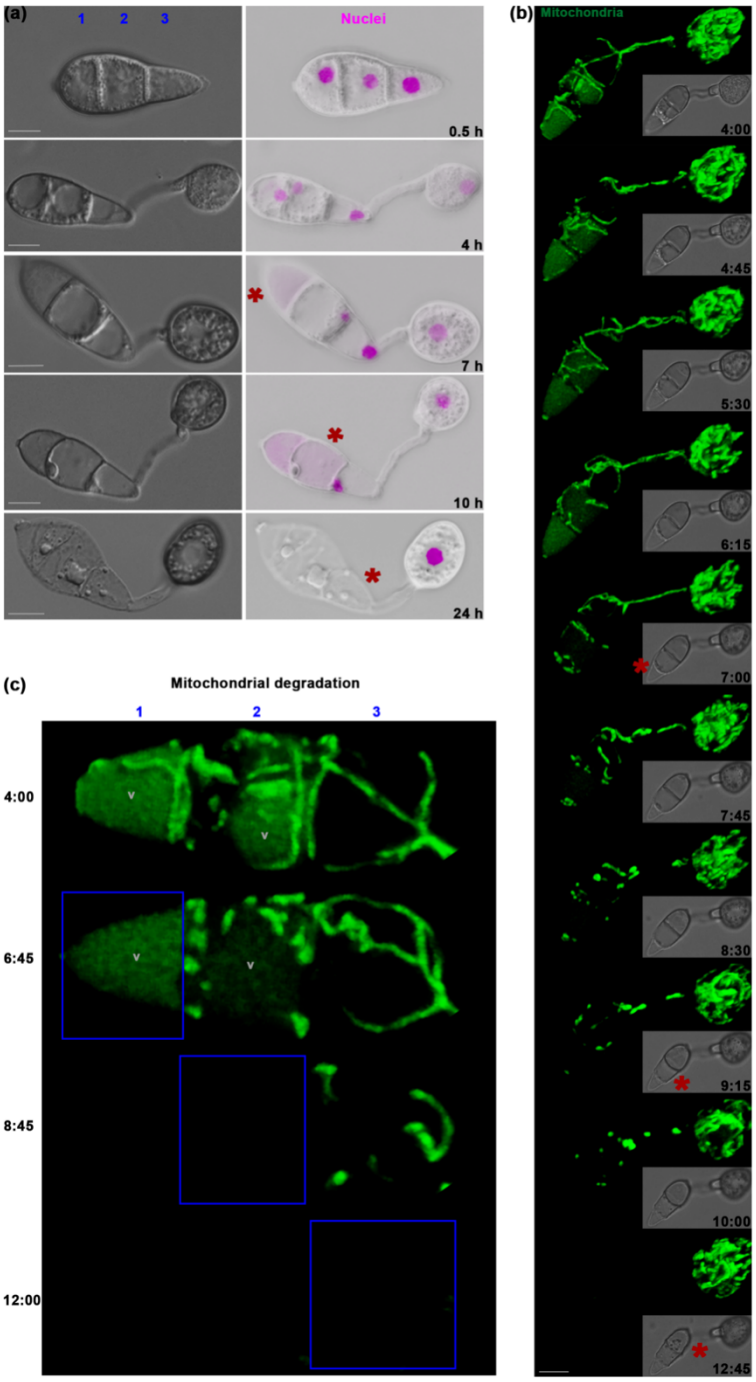

Figure 1. Regulated mitochondrial fission and degradation precede ferroptosis in the conidial cells in *M. oryzae*

(a) *M. oryzae* conidia initiate ferroptosis sequentially during pathogenic development. Conidial cells marked 1,2,3 are terminal, middle, and proximal cells that initiate ferroptotic cell death first, second, and last, respectively. From left to right are the three-celled conidium, germ tube, and appressorium. Red asterisk marks the dead conidial cell, which is also indicated by the disappearance of the nucleus (hH1-GFP, color inverted) in the projection image. DIC images are single plane, and the scale bar equals 5 µm.
(b) Mitochondrial fusion, fission, and degradation along with sequential ferroptosis events. Bright field images are single plane and overlapped in the 3D images of mitochondria displayed by a mitochondrial targeting sequence fused with GFP (MTS-GFP). Red asterisks mark the dead and collapsed conidial cells. Scale bar = 5 µm.
(c) Sequential mitochondrial degradation in the conidium correlates with ferroptosis therein. Mitochondrial degradation finished first in the terminal cell (6:45 hpi), and then in the middle cell (8:45 hpi) and lastly in the proximal cell (12:00 hpi), precisely occurring before the sequential ferroptosis cycle. Blue rectangles highlight the conidial cells that just completed mitochondrial degradation. V denotes the vacuole. Images in **(b)** and **(c)** are from the same time lapse experiment, which is displayed as a montage (Figure S1) and a movie (Supplementary Movie 1). Data shown are representative of 4 replicates of the experiment with similar results. Time depicted as hours post inoculation (hpi) in all the main and supplementary figures.

During the maturation of appressorium, the 3 connected conidial cells undergo ferroptosis individually and sequentially, with the terminal cell dying first, followed by the middle, and lastly the proximal cell (**Figure 1a**)[3]. Little is known about the regulators controlling such precise and highly compartmentalized ferroptosis relay in interconnected cells. Interestingly, a similar sequential behavior prior to ferroptosis was observed for mitochondrial degradation, which commenced and completed first in the terminal cell prior to its collapse and death, and then the same two processes repeated subsequently in the middle and proximal cells around 2 and 5 hours later, respectively (**Figures 1b-c, S1, and Supplementary Movie 1**). Thus, we conclude that the occurrence of ferroptosis specifically correlates with and follows mitochondrial degradation. Thus, the question arose whether and how mitochondria are specifically degraded during ferroptosis? Mitophagy, which targets dysfunctional mitochondria for vacuolar degradation using the autophagy machinery, is one of the pathways responsible for such organellar turnover and homeostasis[4]. Weak free GFP signal in the vacuole (**Figures 1b-c, S1, and Supplementary Movie 1**) implies that mitophagy could be one pathway responsible for the observed mitochondrial degradation and thus led us to examine ferroptosis in the mitophagy mutant, *atg24*Δ[4].

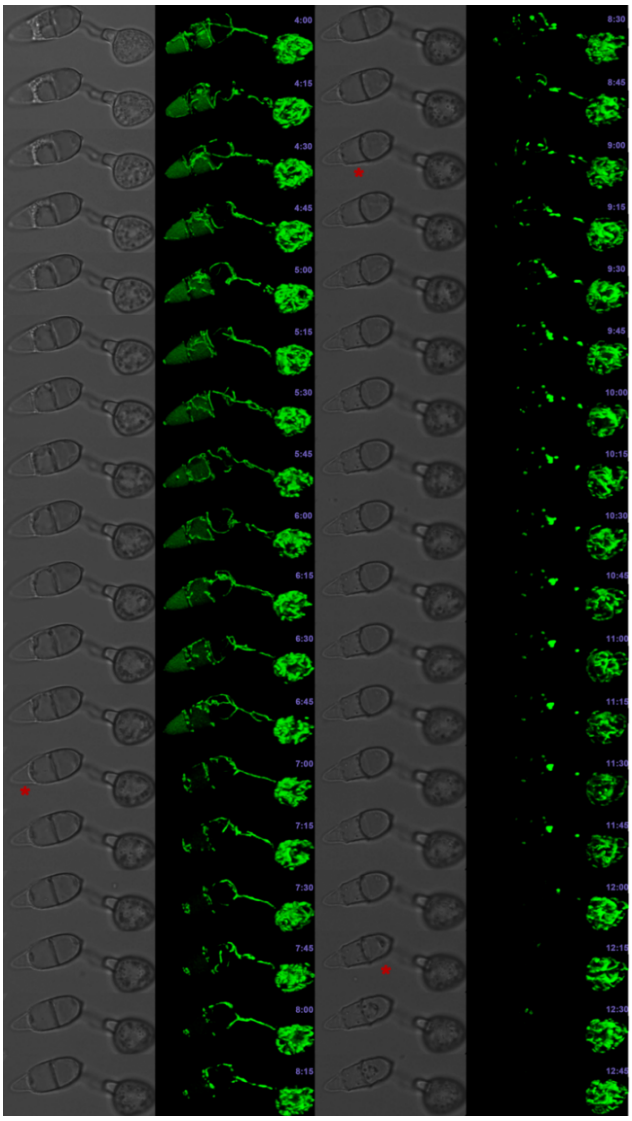

Figure S1.
Montage showing fusion, fission, and degradation of mitochondria along with conidial ferroptosis

Bright field image is single plane while MTS-GFP is shown as a rendered 3D. Collapsing or collapsed/dead conidial cells are highlighted by red asterisks. Time indicated as hpi.

Indeed, loss of mitophagy (**Figure 2a**) significantly suppressed ferroptosis and consequently increased the conidial viability in *atg24*Δ conidia as compared to the wild-type *M. oryzae* (**Figure 2b**). Extensively-fused and dense network of mitochondria was present in the mitophagy-defective *atg24*Δ conidial cells, but was rarely seen in wild-type Magnaporthe conidia wherein the mitophagy is fully functional (**Figure 2a**). Mitophagy was then indirectly disrupted by pharmacologically inhibiting mitochondrial fission thus resulting in stably fused mitochondria that persist and are unable to be cleared due to the larger size and tubular constraints. As expected, disrupting mitochondrial fission led to ferroptosis inhibition in a dose-dependent manner (**Figure 2c**). Likewise, lipid peroxides which drive ferroptosis failed to accumulate along the outer membranes in the *atg24*Δ conidia (**Figure 2d**), and rendered the *atg24*Δ conidia (that consequently lack ferroptosis) incapable of causing blast infection in rice plants (**Figure 2e**) as compared to the wild-type *M. oryzae* isolate. Together, these results confirmed the correlation between ferroptosis and precise vacuolar degradation of mitochondria, thus highlighting an essential role for mitophagy therein, and raised an important question as to what is the exact function of mitophagy during

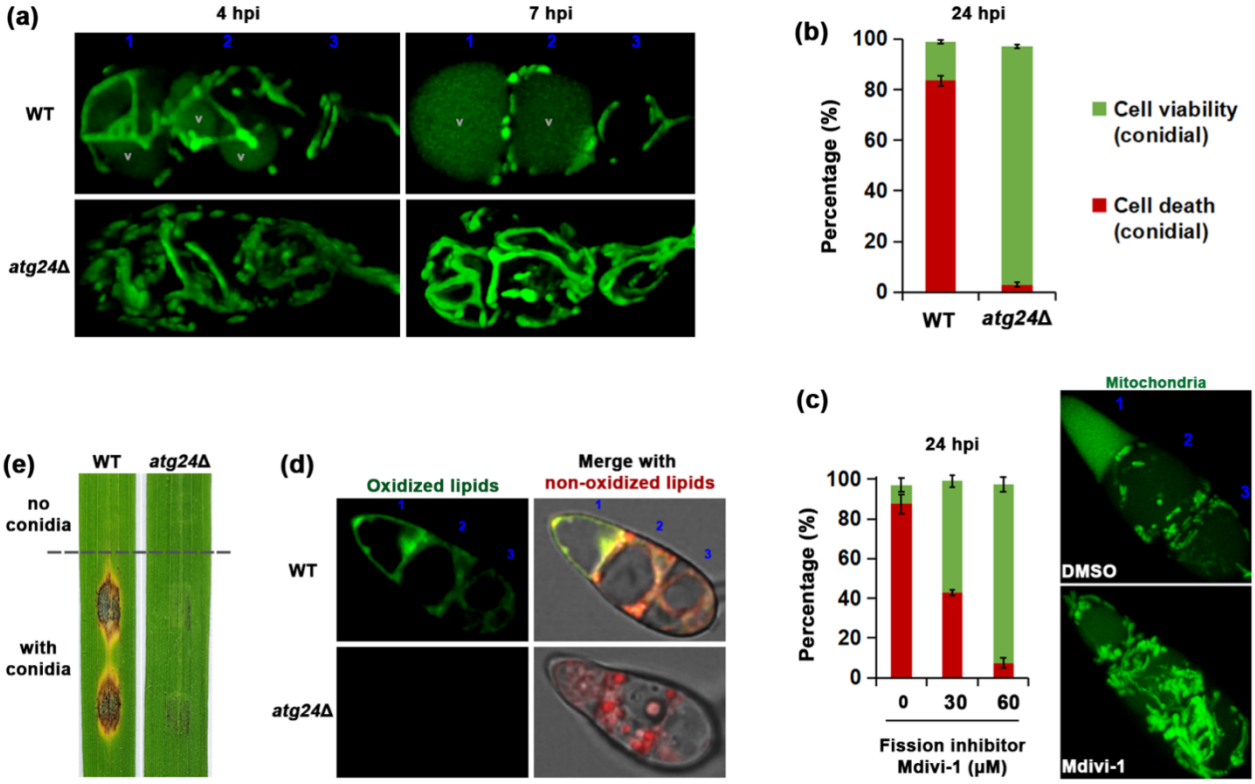

Figure 2. Disruption of mitochondrial degradation via mitophagy suppresses ferroptosis
(a) Mitochondria fuse instead of undergoing degradation when mitophagy is defective. Mitochondria (MTS-GFP shown as 3D images) in wild type (WT) or mitophagy mutant *atg24*Δ were observed at 4 or 7 hpi. V indicates the vacuole. **(b)** Ferroptosis fails to occur in *atg24*Δ conidia. Conidial cell death or viability was quantified at 24 hpi and depicted as mean ± SD from 3 technical replicates, each contains 100 conidia for both wild type (WT) and *atg24*Δ. **(c)** Chemical disruption of mitophagy through Mitochondrial division inhibitor-1 (Mdivi-1) also suppresses ferroptosis in a dose-dependent manner. Mdivi-1 inhibits mitochondrial fission and results in stably fused and persistent mitochondria that cannot be cleared, effectiveness of which on mitochondrial fission was verified by applying it (60 μM) to conidia from 4 hpi, and mitochondrial morphologies observed via MTS-GFP (projection) at 7 hpi. Conidial cell viability or death was quantified at 24 hpi and displayed as mean ± SD (3 technical repeats, n=100 each per dose). **(d and e)** Mitophagy defective *atg24*Δ conidia fail to accumulate lipid

peroxides (oxidized lipids) to a level that can cause ferroptosis, and are defective in ferroptosis-dependent blast disease infection in rice. **(d)** Oxidized (green) and non-oxidized (red) variants of lipids were observed at 7 to 8 hpi via C11-BODIPY$^{581/591}$ staining and ratiometric epifluorescence confocal microscopy and shown as single plane images. **(e)** Rice blast lesions were photographed at 7 days post inoculation. Data in this figure **(a-e)** are representative of 3 independent replicates of the experiment. Quantification in **(b)** or **(c)** is derived from three technical repeats, each with 100 conidia per strain or per dose.

To address this question, mitochondrial metabolism in wild type and *atg24*Δ was examined using the fluorescent dye TMRE whose mitochondrial localization depends on membrane potential, which is in turn also necessary for the import of most precursor proteins into mitochondria[5] thus enabling proper mitochondria metabolism. Shockingly, although a robust filamentous mitochondrial network persisted in the *atg24*Δ conidia, these mitochondria showed a substantial reduction of mitochondrial membrane potential (MMP) as compared to those in the wild-type *M. oryzae* (**Figure 3a**), which indicated that mitophagy is required for maintaining overall metabolic activity likely via recycling dysfunctional mitochondria. Indeed, time lapse imaging showed that all filamentous and punctate mitochondria in the mitophagy-competent wild-type strain, are metabolically active and stain positive with TMRE (**Figure 3b**). Consistent with this observation, localization of the mitochondrial matrix protein Atp1, the α subunit of the F_1 fraction of the ATP synthase, confirmed that mitophagy helps keep and maintain a pool of metabolically active mitochondria prior to initiation of ferroptotic cell death (**Figure 3c**). Together, these data verified the role of mitophagy in maintaining active mitochondria and point out the necessity to understand the relationship between mitochondrial metabolism and ferroptosis.

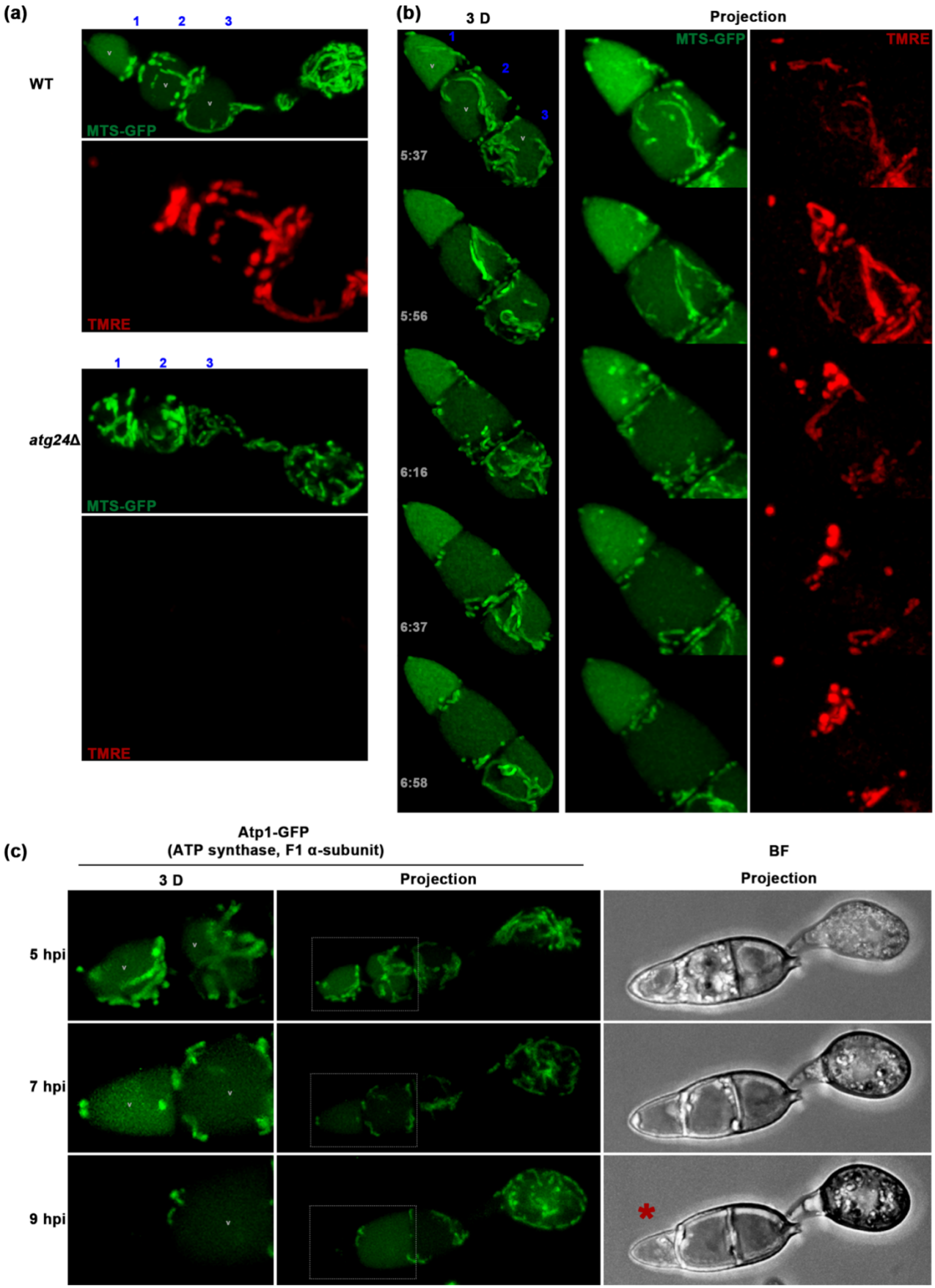

Figure 3. Mitophagy enables and maintains a pool of metabolically active mitochondria
(a) Mitochondrial membrane potential as detected by TMRE staining, is reduced significantly in the *atg24*Δ conidia. MTS-GFP outlines total mitochondria at 6 hpi, along with the corresponding TMRE staining of the conidium. Conidia of wild type (WT) or *atg24*Δ were examined in three independent experiments with at least 30 conidia in total for each strain.

(b) When mitophagy functions properly, both punctuate and filamentous mitochondria are metabolically active and can be stained by TMRE. Time lapse imaging assesses mitochondrial membrane potential along with mitochondrial dynamics from 5:37 to 6:58 hpi. MTS-GFP displayed as 3D rendition or projection outlines total mitochondria, while TMRE stains only metabolically active mitochondria and shows an almost similar distribution pattern as MTS-GFP.
(c) Mitochondria shown by Atp1-GFP, a mitochondrial matrix protein whose import into mitochondria depends on membrane potential. Time lapse imaging from 5 to 9 hpi confirms that mitochondria left by mitophagy machinery are functional and active in metabolism. Gray rectangle marks the origin of the enlarged terminal and middle cells, and the red asterisk marks the collapsed terminal cell. V denotes the vacuole.
Experiments in **(b)** and **(c)** were repeated thrice independently with 6 conidia in each instance.

An indication to such a relationship was provided upon analysis of the mitochondrial β-oxidation mutant *ech1*Δ[6], which has defects in fatty acid oxidative catabolism[6], but showed no obvious defects in mitochondrial membrane potential (**Figure 4a**), and more importantly was capable of undergoing ferroptosis similar to the wild-type *M. oryzae* (**Figure S2**). Differences between *atg24*Δ and *ech1*Δ further suggested that MMP is important and critical for ferroptosis. Such hypothesis was then tested and verified by disrupting the electron transport chain by inhibiting the Complex Ⅲ via antimycin A or by replacing ubiquinone/Coenzyme Q with its analog Idebenone, or by directly decreasing or depolarizing the membrane potential through the protonophore FCCP. Indeed, such treatments caused a significant increase in fused mitochondria and led to a concomitant and significant decrease in ferroptosis (**Figures 4b-c**), akin to the phenotypic defects associated with the loss of mitophagy (**Figures 2a-b**). Working mechanism of Idebenone was further verified and dissected by inhibiting the biosynthesis of ubiquinone via 4-CBA since both may function as an antioxidant and thus potentially inhibit the oxidative stress-dependent ferroptosis[7,8]. Indeed, lower doses of 4-CBA were found to promote ferroptosis and such induction was reversed by the lipophilic antioxidant Liproxstatin-1 (**Figures 4d-e**). However, a higher dose of 4-CBA suppressed ferroptosis (**Figure 4d**), supporting its role in electron transport and thus establishing MMP as an important regulator of ferroptosis in rice blast. Taken together, the above results revealed a requirement of MMP-enabled mitochondrial metabolism in proper and timely induction of ferroptosis. Next, we asked whether mitochondrial metabolism and ferroptotic cell death are functionally linked. ATP synthesis was first tested by promoting glycolysis via exogenous glucose in the low MMP *atg24*Δ or by directly providing ATP in trans. Interestingly, increase in the cellular ATP levels via exogenous supply slightly but significantly increased the conidial cell death in the *atg24*Δ (**Figure 4f**). A similar level of increase was evident regardless of the dosage of glucose or ATP (**Figures 4f and S3**), which further underscored the role of ATP synthesis and mitochondrial metabolism in ferroptosis (**Figure 4g**).

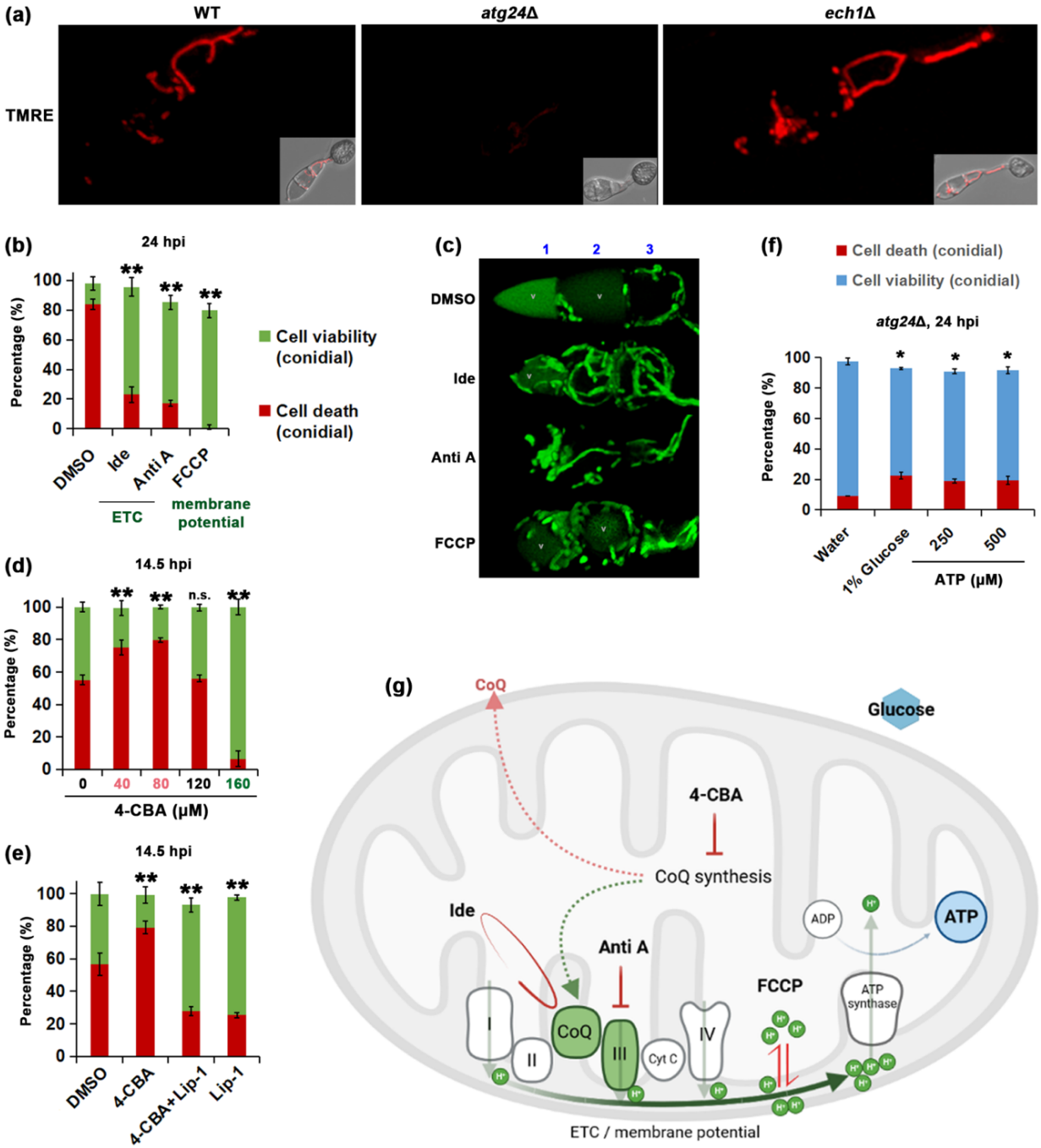

Figure 4. Mitochondrial metabolism is essential for proper ferroptotic cell death in rice blast
(a) A link between mitochondrial metabolism and ferroptosis. Mitochondrial membrane potential (TMRE, only 3 conidial cells are shown) is significantly reduced in *atg24*Δ, but not in the mitochondrial β-oxidation mutant *ech1*Δ, as compared to the wild-type *M. oryzae* (WT). Insets are full view projections merging bright field and TMRE images.
(b) and **(c)** Disruption of electron transport chain or an overall decrease in mitochondrial membrane potential via the protonophore uncoupler/FCCP leads to ferroptosis suppression and mitochondrial fusion. **(b)** Conidial cell viability/death is displayed as mean ± SD from 3 technical replicates with n=100 conidia for each treatment per replicate. **(c)** Mitochondria (MTS-GFP) at 7 hpi are displayed as 3D rendered images. V indicates the vacuole.
(d) Inhibition of Coenzyme Q (CoQ) biosynthesis via exogenous 4-CBA promotes ferroptosis at lower doses, whereas suppresses it at a higher dose. Conidial cell viability or cell death was quantified at 14.5 hpi and is displayed as mean ± SD derived from 3 technical replicates (n=100 conidia each) of the experiment for each dose.
(e) Ferroptosis induction caused by 4-CBA (low dose) is reversed by the lipophilic antioxidant Liproxstation-1 (Lip-1). Conidial cell viability/death presented as mean ± SD (3 technical replicates, n=100 conidia for each treatment per replicate) was quantified at 14.5 hpi.

(f) Ferroptosis defect in *atg24*Δ is only partially suppressed by increasing glycolysis (via glucose) or via exogenous provision of ATP. Conidial cell death (red) or viability (blue) in *atg24*Δ was quantified at 24 hpi, and presented as mean ± SD (3 technical replicates, n=100 conidia for each treatment per replicate).
(g) Schematic model summarizing mitochondria associated processes and their relationship to fungal ferroptosis. Model was created with BioRender.com.
For all, ** ($p < 0.01$) and * ($p < 0.05$) indicate significant differences, while n.s. refers to not significant as compared to the solvent (DMSO or water) control, and data presented have been confirmed through 2 or 3 biological repeats of the experiments.

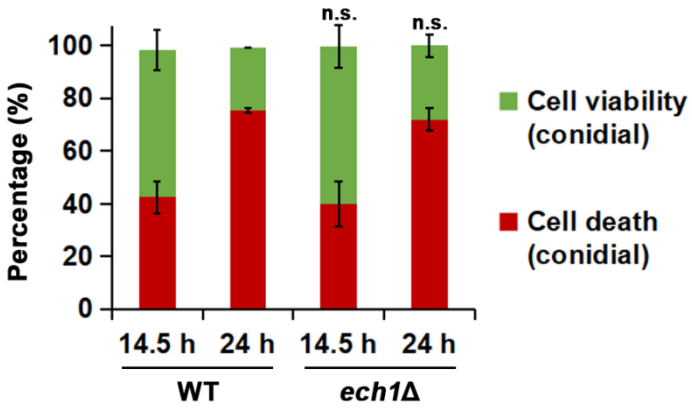

Figure S2. Ferroptotic cell death is normal in the *ech1*Δ conidia.

Conidial cell viability (green) or death (red) in wild type (WT) or *ech1*Δ was quantified at the indicated time points and presented as mean ± SD (3 technical replicates, n=100 conidia for each time point per strain per replicate). n.s. means no significant difference was detected as compared to the WT at the corresponding time points. Experiment has been repeated twice.

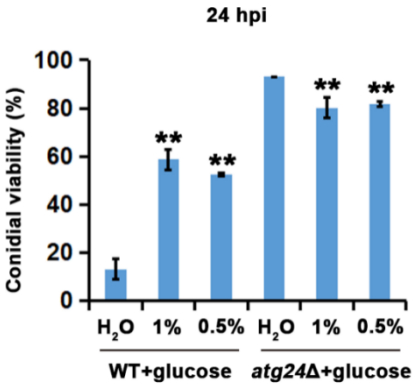

Figure S3. Effect of glucose on conidial viability in the wild-type or *atg24*Δ strain of *M. oryzae*

Conidial viability was quantified at 24 hpi and presented as mean ± SD derived from 3 technical replicates, each containing 100 conidia per treatment per strain. Significant differences detected with or without glucose treatment are marked with ** ($p < 0.01$). This experiment was repeated twice.

Iron deficiency, on the other hand, was repeatedly observed in the *atg24*Δ (**Figure 5a**), which further explains its defect in iron-dependent ferroptosis (**Figures 2b, 2d-e**). However, such iron shortage could not be alleviated by direct iron supplementation (**Figure 5b**), which was intriguing since biosynthesis of the specific source of iron, i.e. the iron-sulfur clusters, in mitochondria and the export of such iron to the cytosol depends entirely on the mitochondrial membrane potential[9,10]. Once cytosolic iron-sulfur cluster levels are low, an iron starvation response is triggered to shut down non-vital iron usage as well as promote iron uptake and release[11]. Not surprisingly, such iron starvation response cannot be bypassed by iron supply if the membrane potential is concurrently diminished in mitochondria. Such MMP-dependent cellular iron control is likely conserved in *M. oryzae,* and thus explains the unique iron-starvation phenotypes observed in the *atg24*Δ mutant in *M. oryzae* (**Figure 5**).

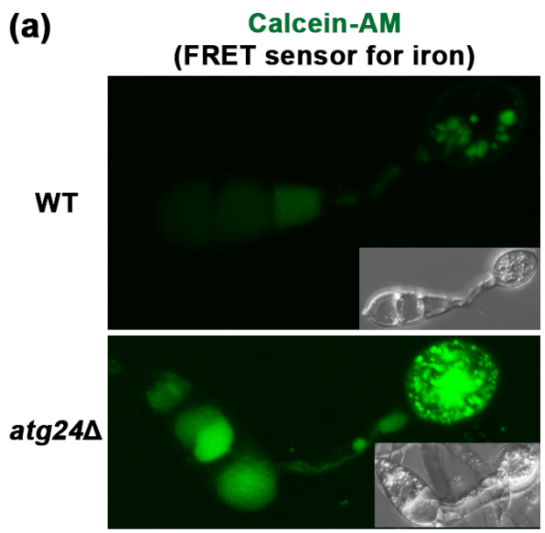

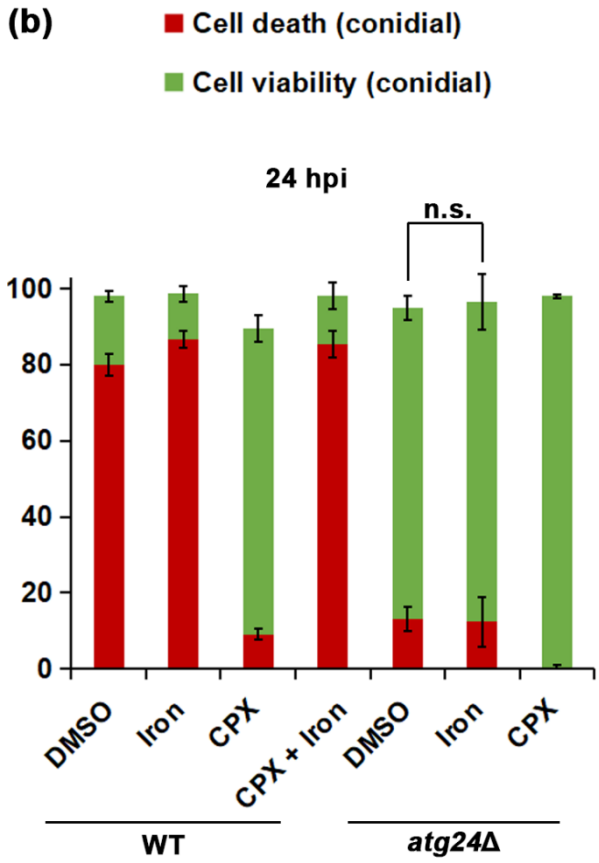

Figure 5. Iron deficiency in the *atg24*Δ cannot be reversed by exogenous supply of iron.

(a) Iron deficiency in *atg24*Δ as shown by the FRET sensor Calcein-AM at 7 hpi. Insets are projection of DIC images.
(b) Ferroptosis defect of *atg24*Δ cannot be suppressed by exogenous iron ($FeCl_3$). Conidial cell death/viability of wild type (WT) or *atg24*Δ in the presence or absence of iron and/or the iron chelator CPX was quantified at 24 hpi and is depicted as mean ± SD, which is derived from 3 technical replicates, each containing 100 conidia per treatment per strain, and n.s. refers to no significant difference. Calcein-AM staining was repeated thrice, whereas the experiments for *atg24*Δ conidial cell death with or without iron or CPX were repeated at least 5 times with similar findings.

In summary, mitophagy is able to distinguish between functional and dysfunctional mitochondria based on low levels of mitochondrial membrane potential and clears such damaged organelles via vacuolar degradation in a precise spatio-temporal manner. Thus, mitophagy is important for ensuring and enabling a pool of metabolically active mitochondria in the viable conidial cells during appressorium formation and maturation. Such active mitochondria are, in turn, necessary for ferroptosis, with the membrane potential-dependent modulation of cellular iron homeostasis,

bioavailability and/or ATP synthesis as potential links connecting these three important processes. Mitochondrial fusion is likely a salvage option to titrate and reduce the negative effects exerted by damaged or dysfunctional mitochondria with reduced membrane potential that are substrates for mitophagy. Together, results here demonstrate an important mitochondrial bioenergetics-based regulatory network for precise ferroptotic cell death in the top-most fungal pathosystem, and provides a likely strategy for intervention of the devastating blast disease in cereal crops.

Materials and Methods

Fungal strains and growth conditions

Magnaporthe oryzae strains were grown on Prune Agar (PA) medium for normal experiment as described[12]. Blast isolate B157 obtained from the Directorate of Rice Research (Hyderabad, India) was used as wild type. Epifluorescence-tagged strains including Histone H1 (hH1)-GFP[3], MTS-GFP[6], Atp1-GFP[6], as well as deletion mutants *atg24*Δ with or without MTS-GFP[4], and *ech1*Δ[6] have been described in our previous publications.

Stains, and confocal microscopy

Sterile water droplets containing freshly harvested conidia at a concentration of 2×10^5 conidia/ml were inoculated on hydrophobic cover glass (Menzel-Glaser) for normal imaging, or a concentration of 1×10^5 conidia/ml were used for inoculating on glass bottom culture dishes (MatTek Corporation, P35G-0-14-C) for time lapse imaging. Roughly 20-30 min before imaging, conidia were stained with 10 µM C11-BODIPY$^{581/591}$ (Thermo Fisher, D3861) to detect lipid peroxidation, or with 250 nM Tetramethylrhodamine ethyl ester perchlorate (TMRE, Sigma, 87917) to assess mitochondrial membrane potential, or 1 µM Calcein-AM (C3099; Invitrogen) for cellular iron.

Laser scanning confocal microscopy was performed using the Leica TCS SP8 X inverted microscope system (Leica Microsystems) under the control of Leica Application Suite X software package (release version 3.5.7.23225). Experiments with C11-BODIPY$^{581/591}$ were done using Matsunami micro slide glass (Matsunami, S7213) and an HCX Plan Apochromat lambda blue 63×/1.20 water immersion objective. Argon laser (excitation, 488 nm; emission, 500-535 nm) was used for the oxidized form whereas the white light laser (excitation, 561 nm; emission, 573-613 nm) was used for non-oxidized variant. HC Plan Apochromat CS2 100× or 63×/1.4 oil immersion objectives and white light laser were used for GFP and Calcein-AM (excitation, 488 nm; emission, 500-550 nm), as well as TMRE (excitation, 540 nm; emission, 580-610nm). All the lasers

associated with Leica TCS SP8 were controlled by the AOTF (Acousto-Optical-Tunable-filter), and fluorescence images were captured using the Leica Hybrid Detector as Z stacks of 10 to 25 sections (0.5 µm-spaced). Time lapse images were further processed using the IMARIS v.9.6.0 software (Bitplane AG, Zurich, Switzerland) to make a movie.

Pharmacological treatment and cell viability/death measurement

Conidia were inoculated on cover glass as above described. 4-Chlorobenzoic acid (4-CBA) (Sigma, 135585) was added at 0 hours post inoculation (hpi), glucose (Duchefa Biochemie, G0802) or ATP (Sigma,A6419) was added at 2.5 hpi, while Mdivi-1 (Sigma, M0199), 32 µM Idebenone (Cayman chemical, 15475), 9.4 µM Antimycin A (Sigma, A8674), 2 µM FCCP (Sigma, C2920), 54 µM liproxstatin-1(Sigma, SML1414), 5 µM ciclopirox olamine (Sigma, C0415), or 5 µM $FeCl_3$ (Sigma, F2877) was added at 4 hpi to maximally restrict the chemical effect on ferroptosis/conidial cell death and minimize the off-target effects on other processes. Conidial cell viability or cell death was quantified using Trypan blue at the indicated time points. Those conidia able to form an appressorium and have 1 to 3 viable conidial cells are considered "viable", while those have a viable appressorium but all the 3 conidial cells are dead are regarded as "dead". Statistical analysis was achieved via Student's *t*-test.

Rice Blast infection assays

The youngest leaf of susceptible CO39 rice seedlings at 4 to 5 leaf stage was used for testing rice infection by wild type or *atg24*Δ, and blast lesion were examined at 7 days after inoculation as previously described[3].

Acknowledgments

We thank the Fungal Patho-Biology Group (TLL, Singapore), Kou Yanjun (CNRRI, China) and Deng Yizhen (SCAU, China) for discussions and useful suggestions. This research was funded by intramural grants from the Temasek Life Sciences Laboratory, Singapore.

Supplementary Data

Supplementary Movie 1: Time-lapse imaging of mitochondrial dynamics and vacuolar degradation during conidial cell death in *Magnaporthe oryzae.* Precise mitochondrial fission and mitophagy precede ferroptotic cell death in each conidial cell in a sequential manner starting with the cell most distal to the appressorium. Mitochondria (MTS-GFP) were monitored from 4 to 12:45 hpi and imaged every 15 min. Merge of MTS-GFP and bright field (BF) is shown as a 3D rendition. The brightness of BF images was manually adjusted to demonstrate the collapse of the dead cells. Supplementary Movie 1 also available at DOI: 10.5281/zenodo.7943903

References

1. Stockwell, B.R. (2022). Ferroptosis turns 10: Emerging mechanisms, physiological functions, and therapeutic applications. Cell *185*, 2401-2421. https://doi.org/10.1016/j.cell.2022.06.003.
2. Shen, Q., and Naqvi, N.I. (2021). Ferroptosis and microbial pathogenesis. PLOS Pathogens *17*, e1009298. 10.1371/journal.ppat.1009298.
3. Shen, Q., Liang, M., Yang, F., Deng, Y.Z., and Naqvi, N.I. (2020). Ferroptosis contributes to developmental cell death in rice blast. New Phytologist *227*, 1831-1846. https://doi.org/10.1111/nph.16636.
4. He, Y., Deng, Y.Z., and Naqvi, N.I. (2013). Atg24-assisted mitophagy in the foot cells is necessary for proper asexual differentiation in *Magnaporthe oryzae*. Autophagy *9*, 1818-1827. 10.4161/auto.26057.
5. SCHLEYER, M., SCHMIDT, B., and NEUPERT, W. (1982). Requirement of a Membrane Potential for the Posttranslational Transfer of Proteins into Mitochondsria. European Journal of Biochemistry *125*, 109-116. https://doi.org/10.1111/j.1432-1033.1982.tb06657.x.
6. Patkar, R.N., Ramos-Pamplona, M., Gupta, A.P., Fan, Y., and Naqvi, N.I. (2012). Mitochondrial β-oxidation regulates organellar integrity and is necessary for conidial germination and invasive growth in *Magnaporthe oryzae*. Molecular Microbiology *86*, 1345-1363. https://doi.org/10.1111/mmi.12060.
7. Doll, S., Freitas, F.P., Shah, R., Aldrovandi, M., da Silva, M.C., Ingold, I., Goya Grocin, A., Xavier da Silva, T.N., Panzilius, E., Scheel, C.H., et al. (2019). FSP1 is a glutathione-independent ferroptosis suppressor. Nature *575*, 693-698. 10.1038/s41586-019-1707-0.
8. Bersuker, K., Hendricks, J.M., Li, Z., Magtanong, L., Ford, B., Tang, P.H., Roberts, M.A., Tong, B., Maimone, T.J., Zoncu, R., et al. (2019). The CoQ oxidoreductase FSP1 acts parallel to GPX4 to inhibit ferroptosis. Nature *575*, 688-692. 10.1038/s41586-019-1705-2.
9. Lill, R., and Freibert, S.-A. (2020). Mechanisms of Mitochondrial Iron-Sulfur Protein Biogenesis. Annual Review of Biochemistry *89*, 471-499. 10.1146/annurev-biochem-013118-111540.
10. Kispal, G., Csere, P., Prohl, C., and Lill, R. (1999). The mitochondrial proteins Atm1p and Nfs1p are essential for biogenesis of cytosolic Fe/S proteins. The EMBO Journal *18*, 3981-3989. https://doi.org/10.1093/emboj/18.14.3981.
11. Volz, K. (2008). The functional duality of iron regulatory protein 1. Current Opinion in Structural Biology *18*, 106-111. https://doi.org/10.1016/j.sbi.2007.12.010.
12. Ramanujam, R., and Naqvi, N.I. (2010). PdeH, a High-Affinity cAMP Phosphodiesterase, Is a Key Regulator of Asexual and Pathogenic Differentiation in *Magnaporthe oryzae*. PLOS Pathogens *6*, e1000897. 10.1371/journal.ppat.1000897.